# An hydrological hazard prevention model for the Alpine region: the case of the Lake Maggiore

M.A. Brovelli(*), M. Cannata(**) and A. Salvetti(**)

(*)Politecnico di Milano, Polo Regionale di Como, via Valleggio 11, 22100 Como, Italy, tel. +390313327517, fax +390313327519, e-mail maria.brovelli@polimi.it
(**)Institute of Earth Sciences, University of Applied Sciences of Southern Switzerland, via Trevano, 6952 Canobbio, Switzerland, tel. +41919351224, fax +41919351209, e-mail massimiliano.cannata@supsi.ch, andrea.salvetti@supsi.ch

## 1 Introduction

In the frame of a European Interreg IIIA project between Italy and Switzerland, named "Development of a hydrological hazard prevention management system in the area of the Lake Maggiore", one of the topic is the set up of an hydrological model to simulate the interaction between artificial reservoirs and the natural rainfall–runoff mechanisms in the watershed. The hydrological model we decided to realise is a distributed, physically based and hourly one.
To accomplish the previous task a database, a statistics package and an interfaced GIS are needed; this software packages are available in the "open source" world (PostgreSQL, R and GRASS) and this was the solution we decided to adopt.
By taking advantage of the interfaces already available between these three packages the hydrological model will be implemented in an interoperable and integrated system.
In other publications problems of input data acquisition, preprocessing and storing related to the hydrological model have been considered. In this work, on the other hand, attention will be focused on certain functionalities of analysis and simulation developed in the integrated environment PostgreSQL, GRASS and R.
To fully implement the rainfall-runoff model, the more relevant hydrological processes have to be accounted for. We started with the simulation of precipitation canopy interception and of evapotranspiration.
In particular methods and algorithms for the creation of climatological and auxiliary thematic maps (i.e.: the temperature, wind velocity and so on for the first, and the height and density of the vegetation for the second) have been worked out. The paper focuses on these topics and presents preliminary results obtained with the new developed commands.
The study area is situated upstream the Lake Maggiore, on the border between Switzerland and Italy. The area is mountainous with elevation ranging from 200 m to about 3500 m a.s.l., particularly prone to heavy rainfall and flood events in spring and autumn, with high variability in space and time.

## 2 Hydrological Modelling and GIS

Hydrological modelling owes its development to the necessity of describing and predicting the changes in the hydrological cycle, often with particular reference to specific processes and variables, among which for example the behaviour of the runoff in a given river section.
Hydrological modelling can therefore be defined as a mathematical representation of hydrological processes capable of providing information of different hydrological variables (groundwater level, soil water content, evapotranspiration, and runoff).

Different models have been developed in the past, aiming at reproducing measured variables or, more often, to predict hydrological processes in ungauged catchments and into the future. However, the final aim of using models is very often to improve decision-making about a hydrological problem, such as flood protection, water resources allocation, etc.
In recent years, given the necessity to evaluate the consequences of environmental changes exacerbated by the effects of human intervention, researchers have turned their attention to an integrated approach to all physical events.
Hydrological modelling is also moving in this direction, developing physically based and spatially distributed models capable of interacting and/or integrating with other interconnected processes.
This kind of modelling calls for the handling of a vast quantity of data and parameters, often coming from different sources and methodologies of measurement corresponding to different spatial and temporal scales.
Because of its advantages of data storage, display and maintenance GIS is a very powerful and promising tool to model the hydrological cycle.
All these requirements have lead to the establishment of links at three different levels between hydrological modelling and Geographic Information Systems (Wesseling et al., 1996):

1 a simple exchange of data (loose coupling);
2 an interface with GIS (tight coupling);
3 an integrated model (embedded coupling).

While for the first level a basic programme for the conversion of formats is enough, the second requires the development within the GIS of an input/output library of the hydrological modelling formats, and the third involves the creation within the GIS itself of hydrological functionalities.
Starting from the 1970s different research groups have been developing distributed physically-based hydrological and transport models.
A reduced set of these models have been further linked to GIS following the loose coupling or tight coupling approach (Burrough, 1996).
Various models can be found at the first two levels of integration with GIS:

- DHSVM (Distributed Hydrology Soil Vegetation Model), originally developed in the early 1990s by Wigmosta at the University of Washington (Wigmosta et al, 1994), available at the web site:
  http://www.hydro.washington.edu/Lettenmaier/Models/DHSVM/index.htm.
  By using a suitable function (myconvert.c) it is possible to convert an ASCII file from GIS ArcInfo into the binary format of the hydrological model; however the output is only displayable by means of the generation of "postscript" images.
- MIKE-SHE developed by the Danish Hydrology Institute DHI (http://www.dhisoftware.com/mikeshe/), which can be integrated with GIS Arcview through the use of an input/output format converter.
- WaSiM, a physically-based hydrological model developed at the Swiss Federal Institute of Technology (ETH) in Zurich has commands for receiving and sending data from and to ArcInfo (http://iacweb.ethz.ch/staff/verbunt/Down/WaSiM.pdf)
- TOPKAPI, a parsimonious physically-based model (Ciarapica and Todini, 2002) those input and output can be directly addressed by GRASS GIS.

The third level of integration between hydrological model and GIS requires the use of an environmental modelling language (EML). This last solution has the advantage that GIS have powerful database and visualization tools and that they manage spatial information. In this view, GRASS is one of the available products.

Completely GIS integrated hydrological models are the following:

- TOPMODEL (http://www.es.lancs.ac.uk/hfdg/topmodel.html), a widely used semi-distributed topographically based model, of which a GRASS version exists (r.topmodel)
- CASC2D (http://www.engr.uconn.edu/~ogden/casc2d/casc2d_home.html) a 2-dimension distributed, physically based model, developed for small catchments in arid or semi-arid environments, where the water infiltration mechanism is mainly of the Hortonian type. In addition to a first level integration with ArcInfo, a completely GRASS integrated version of the model is available (r.hydro.CASC2D).
- LISFLOOD (De Roo et al., 2000) a physically based river basin modelling, written using the PCRaster GIS environment; The PCRaster language is a computer language for construction of spatio-temporal environmental models and supports immediate pre- or post-modelling visualisation of spatio-temporal data (Van Deursen, 1995).

For the purposes of the project we decided to develop a mostly physically based model, built on several independent modules, where single hydrological processes are simulated with concepts that have proven their application, such as the modified Rutter method for interception (Zeng et al., 2000), and the Penman-Monteith method for evapotranspiration (Allen et al., 1998).
As field collected data are essential inputs to the model, but also crucial for model calibration and validation, it is obviously required that the process modelling is tailored to the data available. Further, the adopted process descriptions need to be tailored to the final aims of modelling (Karssenberg, 2002).
Distributed hydrological models require spatial data, both constant parameters and time dependent variables. Basically, traditional data sources provide point or vector data, therefore interpolation techniques are required to produce input maps for hydrological models.
Believing that level three (embedded coupling) is the most appropriate in hydrological modelling, it was decided to move in this direction.
The modelling of the hydrological cycle requires:

1. the availability of accurate meteorological observations (the more complete the better);
2. the use of such observations to interpolate spatial fields;
3. the application of mathematical equations describing the processes to the previously interpolated data;
4. the prediction of the state variables;
5. the accessibility of the results by decision makers responsible for hazard assessment and people safety.

A single integrated environment must offer general tools for storing, accessing, querying and displaying data, statistical and geostatistical functions for validation and processing and specific hydrological tools. In the world of Open Source this multi-faceted system is found in the combination of three software programmes: GRASS (GIS), PostgreSQL (Relational DataBase Management System, RDBMS), and R (Statistics).
In this trio R plays a central role as a point of access for both GIS and RDBMS at a level of total integration: libraries exist within R which allow one to read and write data in the two formats and which make it possible to invoke all the functions present in GRASS and in PostgreSQL (Bivand and Neteler, 2000).

Once defined the development environment, four steps have to be taken into account for the realisation of the GIS hydrological model:

1. the development of automatic procedures for storing and accessing data in the RDBMS;
2. the preprocessing and validation of raw data;
3. the interpolation and elaboration of data for the creation of input maps for the hydrological model;
4. the simulation of the rainfall-runoff process, as a whole.

The first two steps have been already discussed in other publications (Salvetti et al., 2004) or in publications to come. In this paper methods and algorithms for the creation of climatological and thematic maps (i.e.: the temperature, wind velocity and so on for the first, and the height and density of the vegetation for the second) will be presented.
These auxiliary maps are finally used for the simulation of the different hydrological processes, two of which, namely the rainfall canopy interception and the potential evapotranspiration, are presented in details.
The parameterization procedure and preliminary results are presented and briefly discussed in the following paragraphs.

# 3 Data Interpolation and creation of input maps.

Once the valid data is made available, it is necessary to create all the maps required by the different hydrological modules, namely the climatological maps and those of the derived parameters.
Referring to the first, their derivation results from the spatial interpolation of measurements (temperature, humidity, solar radiation, wind velocity, etc) made at control points (meteorological stations). Unfortunately these observation points are few and far between and the investigated phenomenon has a high spatial heterogeneity, which makes difficult the interpretation of the field.
Surface air temperature is an important meteorological input in most formulas for point specific evapotranspiration and snowmelt calculation. Therefore, interpolation of temperature accounting for topography is necessary. Different interpolation schemes were evaluated in literature using the leave-one-outcross-validation method (see e.g. Collins and Bolstad, 1996). The interpolation schemes often applied are:

1. constant lapse rate;
2. inverse distance weighting (IDW) without consideration of elevation effects;
3. ordinary Kriging without consideration of elevation effects;
4. hybrid scheme that combined a constant lapse rate with ordinary Kriging;
5. elevationally detrended kriging approach which is a combination of regression against elevation and ordinary Kriging (Li et al., 2003).

For precipitation and other meteorological variables interpolation the Thiessen's polygons are still widely applied for many applications. IDW and Thiessen methods are both available in GRASS (*s.surf.idw* command).
We investigated different techniques and the influence on the temperature of various parameters: the elevation ($Z$) was found as the most significant one. As balance between accuracy and simplicity, we decided to focus on an elevation dependent interpolation procedure. Therefore we test three models:

1. a linear variation with height with constant lapse rate:

$$T = aZ + b \quad (1)$$

2. a second order polynomial function, which takes into account possible inversion phenomena during the winter season:

$$T = aZ^2 + bZ + c \quad (2)$$

3. a second order polynomial in X and Y with a term in Z, following the results of Collins (Collins and Bolstad, 1996):

$$T = b + b_1X + b_2Y + b_3X^2 + b_4Y^2 + b_5XY + b_6X^3 + b_7Y^3 + b_8X^2Y + + b_9XY^2 + b_{10}Z \quad (3)$$

The mean absolute error for each model was investigated with a leave-one-outcross-validation method procedure for the whole 2002 year and the results, shown in table 1, reveal that model 1 gives the worst predictions while model 2 and 3 are quite similar and therefore both suitable for temperature interpolation.
First at each time step the parameters of the two linear models are estimated using the R linear modelling command *lm()*, then the mean error predictions are evaluated using a cross-correlating technique and finally the more appropriate linear model, by means of the GRASS map algebra command (*r.mapcalc*), is applied in order to derive the temperature (figure 1). This interpolation scheme is automatically implemented within R using the provided programming capability.
The scheme adopted is objective, since the relationship between temperature and elevation is established through ground measurements at each calculation time step.

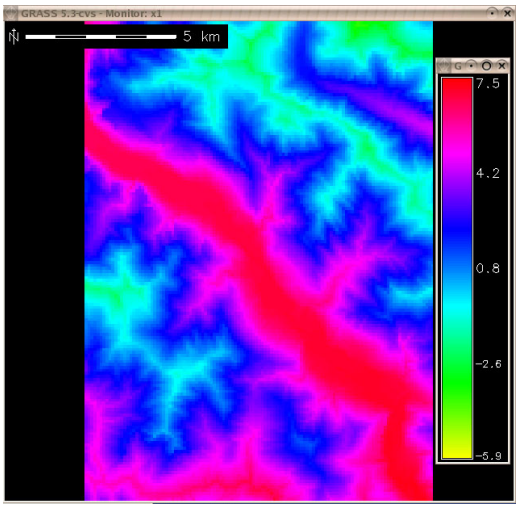


Figure 1: Temperature map

| | | Linear with Z (1) | Second order polynomial in Z (2) | Second order polynomial in X,Y with a term in Z (3) |
|---|---|---|---|---|
| **MAE** | **Max** | 5.815 | 5.832 | 195.589 |
| | **Min** | 0.427 | 0.440 | 0.418 |
| | **Average** | 1.530 | 1.522 | 4.368 |
| | **Median** | 1.353 | 1.345 | 1.778 |

Table 1: Mean Absolute Error Statistics of 3 different temperature interpolation models

# 4 Simulation of the rainfall-runoff process

The model under development is a mostly physically based model, defined by a regular horizontal grid of user defined size. Mass and energy budget are solved for each cell, by considering the most relevant processes of the water cycle (rainfall/snowfall, interception, evapotranspiration, infiltration, runoff formation and transfer on slopes and in the drainage network). In the vertical dimension the model will consider surface, subsurface and groundwater flow. In the river channel network a kinematic wave approach is used, as proposed in the TOPKAPI model.
Model inputs are meteorological data (precipitation, temperature, wind velocity, global radiation, etc). This data has to be spatially interpolated, in order to account for variability inside the catchment. Moreover land use, *LAI* (Leaf Area Index), soil type and texture, soil depth are required to completely parameterize the catchment.

# 5 Thematic maps

To model the previously mentioned processes some parameter maps have to be derived, mainly based on land use, soil properties and topography.
For radiation exchange between earth surface and atmosphere the albedo ($a$) of different surfaces and the Linke Turbidy factor ($L_{tf}$) are required.
For the evapotranspiration process the type, the state and the energy interaction between the atmosphere and the vegetation in terms of *LAI*, the height of vegetation ($V_h$), the density of the canopy ($V_c$), the minimal superficial resistance of the vegetation ($R_{sc}$) must be considered.
The solutions chosen for the creation of the maps of *LAI*, $V_h$ and $V_c$, according to the WaSiM model approach (Schulla, 1997), calculate the raster map on the basis of values associated with four specific days of the year and relative to a reference height of 400 m a.s.l. (from $[d_{1,400}]$ to $[d_{2,400}]$ of the growing season and from $[d_{3,400}]$ to $[d_{4,400}]$ of the dormant season) and relative to different land uses.
Keeping in mind the existence of a temporal shift as a function of altitude ($h$), it is possible for each cell of the model to calculate the values:

$$d_{i,h} = d_{i,400} + 0.025 \cdot (h - 400) \tag{4}$$

being $i$ = [1,2,3,4] the index of the four reference days and $h$ the height above sea level of the cell.
By means of the linear interpolation it is possible to compute the value assumed by *LAI*, $V_h$ and $V_c$ cell by cell.
On the other hand, $a$, $R_{sc}$ and $L_{tf}$ do not undergo any variation with elevation and their mean monthly values are available in the literature according to the different land uses. In this case the maps do not depend on the elevation, but only on the date and on the land use.
While for the first three maps (*LAI,* $V_h$, $V_c$) the process for the creation of maps has been automated by the command *f.par2rst* in GRASS, for the second three ($a$, $R_{sc}$, $L_{tf}$) a dedicated R script has been created by using the *r.mapcalc* command.

# 6 The evapotranspiration

The evaporation consists in the conversion of water from the liquid to the vapour state. This physical process is controlled both by the energy availability on the evaporating surface and by the facility with which the water vapour can be diffused in the atmosphere. Methods differing from the specific data availability (temperature, global radiation, wind velocity, etc.) and from the temporal resolution (hourly up to several days) have been developed and can be found in literature (Shuttleworth, 1992).

The approach we decided to adopt to calculate the evapotranspiration is the one from FAO (Allen et al., 1998) which recommends the use of the equation of Penman-Monteith. The strength of the original formulation of Penman (Penman, 1948) lies in combining the energy budget with the transport of mass in the calculation of the evaporation from a water surface as a function of solar radiation, temperature, humidity and wind velocity. Later on Monteith (Monteith, 1965) introduced two factors of resistance which allow to extend the validity of the solution to vegetated areas: the first factor is the aerodynamic resistance taking into account the friction of the air on the vegetation while the second one is the superficial resistance representing the difficulty for the vapour to pass through the stomata, the leaf surface and the soil.
Therefore for the vegetated areas hourly potential evapotranspiration is calculated by the Penman-Monteith's formula, (which is a sum of radiative (*ETrad*) and aerodynamic terms (*ETaero*)) while for water surfaces the evaporation is computed by using the original Penman's formula (containing the single aerodynamic term).
The choice of this method to estimate the evapotranspiration is based on the fact that:

- the Penman-Monteith method requires, unlike other methods, neither a local calibration nor the definition of the wind field on the basis of the observations and therefore it allows us to compare data from various zones;
- the Penman-Monteith method is based on physical considerations and explicitly contains the parameters describing both physiological and aerodynamic components;
- the results of the studies by many authors summarized in the document of the experts of FAO (Allen at al., 1998), suggest to use the Penman-Monteith method for the determination of the potential evapotranspiration.

Being:

| | | |
|---|---|---|
| $\lambda$ | = | latent heat of vaporisation; |
| $\Delta$ | = | slope of vapour pressure curve; |
| $\gamma$ | = | psychrometrics constant; |
| $\gamma^*$ | = | modified psychrometric constant (depending on $r_s$ and $r_a$); |
| $\rho$ | = | atmospheric constant; |
| cp | = | specific heat of moist air; |
| $r_s$ | = | bulk surface resistance (see Fig. 1); |
| $r_a$ | = | aerodynamic resistance (see Fig. 1); |
| $e_s$ | = | mean saturation vapour pressure; |
| $e_a$ | = | actual vapour pressure; |
| $R_n$ | = | net radiation; |
| G | = | soil heat flux; |
| $u_2$ | = | windspeed at 2 meters height; |

the Penman-Monteith equation for a vegetated surface is:

$$\begin{cases} ETp = ETrad + ETaero \\ ETaero = \dfrac{0.001}{\lambda}\dfrac{1}{\Delta+\gamma^*}\dfrac{\rho\cdot cp}{r_a}\left(e_a - e_s\right) \\ ETrad = \dfrac{\Delta}{\Delta+\gamma^*}\dfrac{R_n - G}{\lambda\cdot 1E6} \end{cases} \quad (5)$$

In case of water surface the original Penman equation is:

$$\begin{cases} ETaero = 0.035 \cdot \left(0.5 + \dfrac{0.621375 \cdot u_2}{100}\right) \cdot 7.500638 \cdot \left(e_a - e_s\right) \\ ETp = \dfrac{\left(R_n \cdot \lambda \cdot \Delta\right) + \left(\gamma \cdot ETaero\right)}{\Delta + \gamma} \end{cases} \quad (6)$$

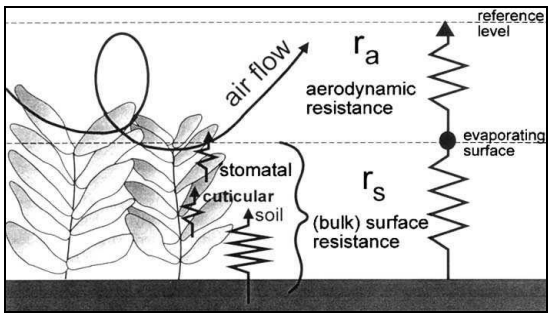


Figure 2 – Evapotranspiration process schema after FAO (1998)

The most important parameter to be considered in the energy budget is the net solar radiation. The factors that determine the differences in the radiative budget are the albedo (the fraction of short-wave radiation reflected by the earth's surface) and the air temperature (determining the long-wave radiation).
For this purpose the *r.sun* GRASS command was used, which computes direct, diffuse and ground reflected solar radiation for a given day, latitude, surface and by clear sky condition, giving the possibility to consider the shadow due to the topography and the attenuation effect due to the turbidity of the atmosphere. By specifying the ground albedo and the turbidity map, the solar radiation in clear sky condition is obtained. Another effect attenuating the energy coming from the sun to the earth surface is cloudiness. An index of this phenomenon can be obtained at each meteorological station by computing the ratio between measured and clear sky radiation.
By using the interpolation map of this ratio it is possible to obtain the map of net solar radiation.
All these procedures have been implemented by means of a R script invoking the GRASS commands *r.sun*, *s.idw.rst*, *r.mapcalc* and the new command *r.evapo.PM*.
In figure 3 it is possible to see the strong influence of the clear sky index, on the estimated evapotranspiration: two maps of ETp at the same hour in two following days with respectively low and high cloudiness index are showed.

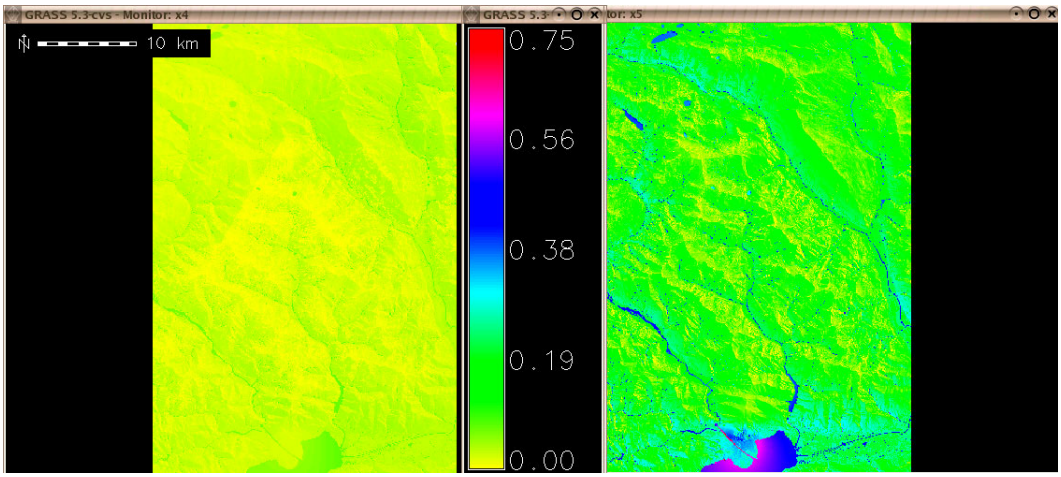


Figure 3: Estimated hourly evapotranspiration in a cloudy day (left) and in a sunny day (right).

## 7 The canopy interception

Canopy interception plays an important role in determining the amount of rainfall reaching the soil surface. During a rainfall event, water either penetrates the canopy falling directly to the soil, or is intercepted by the canopy. From there it can drip to the ground surface, flow down tree stems, or be held and evaporated. The portion that falls directly to the ground or drips from the canopy is termed throughfall. Rainfall that is intercepted and flows down the tree trunk is known as stemflow, and the remainder is called interception.
The amount of rainfall intercepted by a forest canopy depends on storm size, intensity, duration, rainfall frequency, forest structure, tree species, age, and density. Depending on all these conditions, canopy interception can account for 15 to 35% of annual rainfall, although the influence during intense storm event is obviously more reduced.
The first physically based method for canopy interception estimation was proposed by Rutter (Rutter at al., 1971) being the basis of numerous subsequent analytical model. It models the canopy by means of a storage described by a maximum storage capacity ($C_m$), filled by precipitation ($P$) and dried by evaporation ($IL$) and by drainage ($D$), depending on the current storage level ($C_a$).
As noted by Zeng (Zeng et al., 2000), rainfall temporal characteristic is an important factor on the interception loss; in fact:

- heavy rains quickly saturate the canopy storage as consequence of the low maximum storage capacity values;
- low rains produce higher interception loss values than the heavy ones;
- the amount of evaporated water depends on the time interval between two following rainfall events.

An analytical model has been therefore derived and the new command *r.interception* has been implemented in GRASS.
The exceeding water is assumed to drain instantaneously from the canopy storage. Therefore D is modelled by the following equation:

$$D = \begin{cases} \infty & C_a > C_m \\ 0 & C_a \le C_m \end{cases} \tag{7}$$

The water balance for the canopy storage is modelled following the equation:

$$\frac{\partial C_a}{\partial t} = P - IL - D \tag{8}$$

where *IL* (called interception loss) is:

$$IL = \left( \frac{C_a}{C_m} \right) \cdot ETp \tag{9}$$

with *ETp* = evaporation from a water surface, computed with the command *r.evapo.PM*.
As shown in figure 4, the dynamic of the canopy storage level is described by three different phases: the wetting, the saturation and the drying one.

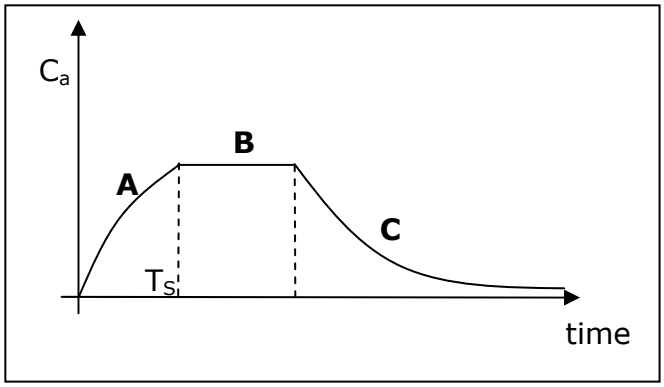


Figure 4 – Canopy storage phases: wetting (A), saturation (B) and drying (C).

Considering a constant rainfall intensity (*P*) during a single time step [$T_0$ ,*T*] and knowing the relative values of $C_a(T_0)$ and *ETp*:

- if *P*>0 e $C_a(T_0) = C_m$ we are in a saturation phase and the interception loss are evaluated by:

$$IL = ETp \cdot T \; ; \tag{10}$$

- if *P*=0 e $C_a(T_0) \neq 0$ we are in a drying phase and the interception loss is evaluated by:

$$IL = C_a \cdot \left[ 1 - \exp\left( - \frac{T \cdot ETp}{C_m} \right) \right]; \tag{11}$$

- if *P*>0 and $C_a(T_0) < C_m$ and $P_s > P$, where $P_s$ is the rainfall intensity that brings the storage level at saturation at the end of the step (time *T*), we are in a wetting phase and the interception loss is evaluated by:

$$IL = P \cdot T - \left[ C_a(T) - C_a(T_0) \right]; \tag{12}$$

- if *P*>0 and $C_a(T_0) < C_m$ and $P_s < P$, we are in a mixed phase of wetting and saturation, being $T_s$ the time when saturation is reached. The interception loss is evaluated by:

$$IL = P \cdot T_S - \left[ C_m - C_a(T_0) \right] + (T - T_S) \cdot ETp \; ; \tag{13}$$

Solving together equations (6), (7) and the appropriate among (9)-(12), it is possible to evaluate at the end of the time step the drainage, the interception loss, and the canopy storage level. Applying the fraction of vegetation covering each sample area (which must be large enough to include the canopy and inter-canopy space but small enough to assure rainfall homogeneity) the *r.interception* command produces three output raster maps (*IL*, *D* and $C_a(T)$).

# 8 Preliminary results

In order to verify the reliability of the developed procedures the entire module, previously described, was run over 360 consecutive hours with measured data of May 2004. At each time step output raster maps of several variables were produced and further sampled in different points of the study region, according to different exposition, height, land use and other characteristics.
In table 2 the minimum, maximum and mean values are summarized in order to show the range of the estimated variables.

| | mean | max | min | unit |
|---|---|---|---|---|
| Rain | 0.40 | 9.00 | 0.00 | [mm/h] |
| Wind speed | 2.11 | 9.90 | 0.10 | [m/s] |
| Humidity | 0.14 | 1.14 | 0.00 | [%] |
| Temperature | 6.37 | 23.55 | -7.57 | [°C] |
| LAI | 4.49 | 9.95 | 1.00 | [-] |
| Vegetation height | 4.33 | 10.00 | 0.10 | [m] |
| Vegetation cover | 0.75 | 0.90 | 0.10 | [-] |
| Albedo | 0.14 | 0.20 | 0.05 | [-] |
| Net radiation | 0.46 | 4.49 | -2.82 | [MJ/(h *$m^2$)] |
| Potential evapotranspiration | 0.08 | 0.92 | 0.00 | [mm/h] |
| Potential evaporation | 0.14 | 1.38 | 0.00 | [mm/h] |
| Interception loss | 0.02 | 0.40 | 0.00 | [mm/h] |
| Interception drainage | 0.38 | 8.99 | 0.00 | [mm/h] |
| Canopy storage level | 0.67 | 3.34 | 0.00 | [mm/h] |

Table 2: Sampled points statistic of major variables.

In figure 5 the temporal behavior of the variables at one selected point is showed. The first part of the period was characterized by wetting conditions, with two short rainfall events and a long lasting 4-days event with a total amount of 81.5 mm. On the opposite, in the second part of the period early summer conditions were measured, with relative high temperature and no cloud cover for several days.
According to this input dataset the evapotranspiration both from water surface and vegetation was calculated. The typical diurnal cycle of the process is well reproduced in figure 5; the influence of the cloud cover during the first days which reduces the radiation amount available for evapotranspiration is also evident.
By clear sky conditions evaporation values up to 0.7 mm/h are predicted from water surfaces; cumulative daily values of 4.2 and 2.2 mm are calculated respectively for water and for vegetated surfaces: these are in good agreement with other previous estimates in the study region (Menzel, 1997).
Concerning interception, the pattern of the water drained from vegetation is quite similar to that of rainfall, due to the large amount of measured rainfall, compared with the small volume available as storage in the canopy.

Significant losses by evaporation from wet leaves can be observed both during heavy and moderate rainfall events, which are also confirmed by the depletion of the interception storage after the events.
On the whole, the obtained results both for evapotranspiration and interception can be regarded as well promising; a more detailed validation procedure, with a longer data set, is main part of future work.

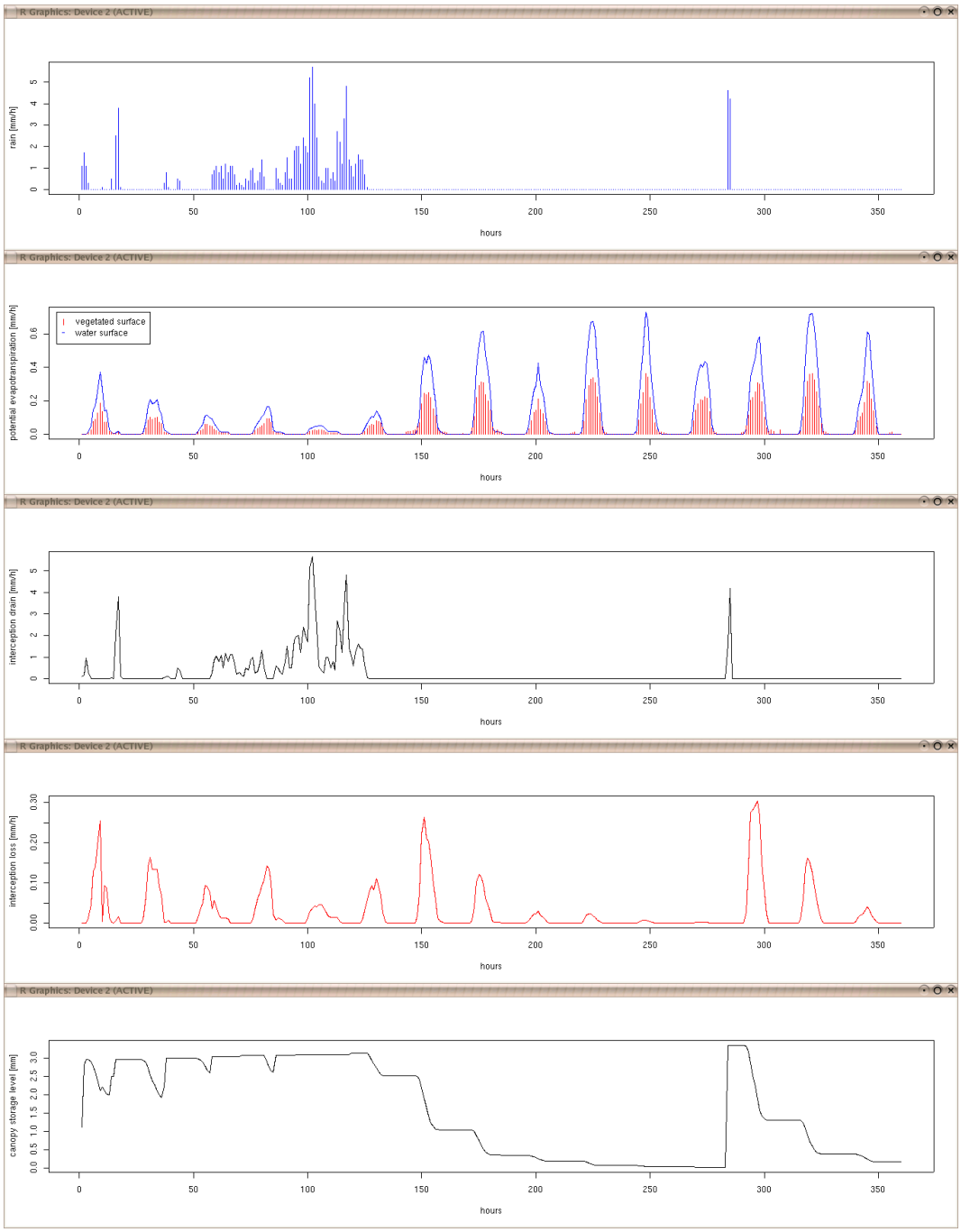


Figure 5: temporal behavior of the modeled variables at one selected point (from top to bottom: rain, evapotranspiration and evaporation, interception drainage, interception loss and canopy storage level).

# 9 Conclusion

In the frame of the European project "Development of a hydrological hazard prevention management system in the area of the Lake Maggiore" an approach that combines precipitation analysis with RDBMS-GIS application and hydrological modeling to predict flood potential is being carried out.
The backbone of the system was found in interfacing three freeware and open source software programmes: GRASS (GIS), PostrgreSQL (Relational DataBase Management System, RDBMS), and R (Statistics).
Within this integrated system a distributed and mostly physically based model is being developed by means of several independent and high valued functions, where single hydrological processes are simulated with concepts that have proven their application, such as the modified Rutter method for interception and the Penman-Monteith method for evapotranspiration.
In the paper these commands and the first results have been presented.

# References

[1] Allen R. G., Pereira L.S., Raes D., Smith M. FAO Irrigation and Drainage Paper No. 56 Crop evapotranspiration (guidelines for computing crop water requirements). 290 pages, ISBN 92-5-104219-5, 1998.

[2] Bivand, R., Neteler, M. Open Source geocomputation: using the R data analysis language integrated with GRASS GIS and PostgreSQL data base systems, 2000.

[3] Burrough, P.A. Opportunities and limitations of GIS-based modeling of solute transport at the regional scale. D.L. Corwin and K. Loague (eds), 1996.

[4] Ciarapica, L., Todini, E. TOPKAPI: a model for the representation of the rainfall-runoff process at different scales, *Hydrological Process*es 16, pages 207-229, 2002.

[5] Collins, F. C, Bolstad, P. V., "A comparison of Spatial Interpolation Techniques in Temperature Estimation", http://www.ncgia.ucsb.edu/conf/SANTA_FE_CD-ROM/sf_papers/collins_fred/collins.html , 1999.

[6] De Roo, A.P.J., Wesseling, C.G., Van Deursen, W.P.A. Physically-based river basin modelling within a GIS: The LISFLOOD model. *Hydrological Processes*, 14, pages 1981-1992, 2000.

[7] Karssenberg, D. The value of environmental modelling languages for building distributed hydrological models: Hydrological Processes, v. 16, p. 2751-2766, 2002.

[8] Li, S., Tarboton D. and McKee M. GIS-based temperature interpolation for distributed modeling of reference evapotranspiration", 23rd AGU Hydrology Days, Fort Collins, Colorado, March 31 - April 2, 2003.

[9] Menzel L. Modellierung der Evapotranspiration im System Boden-Pflanze-Atmosphäre, PhD Dissertation, Federal Institute of Technology Zurich, Geographical Institute Book No. 67 (in german), 1997.

[10] Monteith, J.L. 1965. Evaporation and the environment. 205-234. In the movement of water in living organisms, XIXth Symposium. Soc. of Exp. Biol., Swansea, Cambridge University Press.

[11] Penman, H.L., Natural evaporation from open water, bare soils, and grass, Proc. Roy. Meteorol. Soc. A., 193, 120ff, 1948.

[12] Rutter, A. J., Kershaw K.A., Robins P.C., and Morton A.J., 1971: "A predictive model of rainfall interception in forests: I. Derivation of the model from observations in a plantation of Corsican ine",Agric. Meteorol. 9, pages 367-384.

[13] Salvetti, A., Cannata, M., Brovelli, M.A., Mastropietro, R., Flood forecasting and warning system for the Lake Maggiore area, Southern Switzerland, Abstract Proceedings of the 4th Annual Meeting of the European Meteorological Society, Nice, 26-30 September 2004.

[14] Schulla, J. Hydrologische Modellierung von Flussgebieten zur Abschätzung der Folgen von Klimaänderungen. Zürcher Geographische Schriften 69, ETH Zürich, 187 pages, 1997.

[15] Shuttleworth, W. J., "Evaporation," Chapter 4 in Handbook of Hydrology, Edited by D. R. Maidment, McGraw-Hill, New York, 1992.

[16] Van Deursen, W.P.A. Geographical Information Systems and Dynamic Models: development and application of a prototype spatial modelling language. Doctor's dissertation, Utrecht University, NGS 190, 1995.

[17] Wesseling, C.G., D. Karssenberg, W.P.A. van Deursen, and P.A. Burrough. Integrating dynamic environmental models in GIS: The development of a Dynamic Modelling language. Trans. GIS 1:40–48., 1996.

[18] Wigmosta, M. S., Vail, L. W., and Lettenmaier, D. P. A distributed hydrology vegetation model for complex terrain. *Water Resources Research*, 30(6):1665–1679, 1994.

[19] Zeng , N., J.W. Shuttleworth, J.W., J.H.C. Gash, J.H.C. Influence of temporal variability of rainfall on interception loss. Part I. Point analysis", Journal of Hydrology 228, pages 228-241., 2000.